Electrophoresis of a Colloidal Sphere in a Spherical Cavity with Arbitrary Zeta Potential Distributions

ARTICLE *in* LANGMUIR · AUGUST 2007

Impact Factor: 4.46 · DOI: 10.1021/la7004002 · Source: PubMed

2 AUTHORS, INCLUDING:

Huan J. Keh
National Taiwan University
188 PUBLICATIONS **2,594** CITATIONS

Langmuir

Research Article

Electrophoresis of a Colloidal Sphere in a Spherical Cavity with Arbitrary Zeta Potential Distributions

Huan J. Keh, and Tzu H. Hsieh

Langmuir, **2007**, 23 (15), 7928-7935 • DOI: 10.1021/la7004002

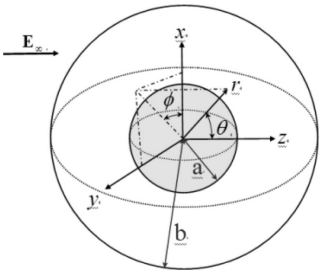

$$\mathbf{U} = \frac{\varepsilon}{4\pi\eta}[\alpha_{\mathrm{p}}(M^{\mathrm{p}}\mathbf{I} - \frac{1}{2}\mathbf{Q}^{\mathrm{p}}) + \alpha_{\mathrm{w}}(M^{\mathrm{w}}\mathbf{I} - \frac{1}{2}\mathbf{Q}^{w})]\cdot\mathbf{E}_{\infty}$$

$$\mathbf{\Omega} = \frac{9\varepsilon}{16\pi\eta a}[\gamma_{\mathrm{p}}\mathbf{D}^{\mathrm{p}} + \gamma_{\mathrm{w}}\mathbf{D}^{w}]\times\mathbf{E}_{\infty}$$

More About This Article

Additional resources and features associated with this article are available within the HTML version:

- Supporting Information
- Links to the 2 articles that cite this article, as of the time of this article download
- Access to high resolution figures
- Links to articles and content related to this article
- Copyright permission to reproduce figures and/or text from this article

View the Full Text HTML

Articles

Electrophoresis of a Colloidal Sphere in a Spherical Cavity with Arbitrary Zeta Potential Distributions

Huan J. Keh* and Tzu H. Hsieh

Department of Chemical Engineering, National Taiwan University, Taipei 10617, Taiwan, Republic of China

Received February 11, 2007. In Final Form: May 7, 2007

An analytical study is presented for the quasi-steady electrophoretic motion of a dielectric sphere situated at the center of a spherical cavity when the surface potentials are arbitrarily nonuniform. The applied electric field is constant, and the electric double layers adjacent to the solid surfaces are assumed to be much thinner than the particle radius and the gap width between the surfaces. The presence of the cavity wall causes three basic effects on the particle velocity: (1) the local electric field on the particle surface is enhanced or reduced by the wall; (2) the wall increases the viscous retardation of the moving particle; and (3) a circulating electroosmotic flow of the suspending fluid exists because of the interaction between the electric field and the charged wall. The Laplace and Stokes equations are solved analytically for the electric potential and velocity fields, respectively, in the fluid phase, and explicit formulas for the electrophoretic and angular velocities of the particle are obtained. To apply these formulas, one has to calculate only the monopole, dipole, and quadrupole moments of the ζ-potential distributions at the particle and cavity surfaces. It is found that the contribution from the electroosmotic flow developing from the interaction of the imposed electric field with the thin double layer adjacent to the cavity wall and the contribution from the wall-corrected electrophoretic driving force to the particle velocities can be superimposed as a result of the linearity of the problem.

1. Introduction

Electrophoresis refers to the motion of a charged particle in an electrolyte solution subject to an applied electric field. Most colloidal particles bear charges on their surfaces as a consequence of the dissociation of functional groups or crystal lattice defects when immersed in an ionic solution. The counterions in the solution are attracted by the surface charge of the particle so that their concentration becomes higher in the vicinity of the particle surface than the bulk value. However, the co-ions are repelled from the particle surface. Hence, a region of mobile ions that is not electrically neutral forms, surrounding the particle. The combination of this region and the fixed charge on the particle surface is well known as an electric double layer. When an external electric field is imposed, the interaction between the particle's surface charge and this field drives the particle to migrate at an electrophoretic velocity in one direction, whereas the counterions in the double layer move in the opposite direction, inducing an ambient fluid flow field different from that caused by the sedimentation of the particle. Electrophoresis has long been used as an effective technique for the separation and identification of biologically active compounds in the biochemical and clinical fields.

A simple expression for the electrophoretic velocity of a dielectric particle of arbitrary shape is the Smoluchowski equation,[1−3]

$$\mathbf{U}_0 = \frac{\epsilon\zeta_p}{\eta}\mathbf{E}_\infty \tag{1}$$

where ζ_p is the ζ potential on the particle surface, η is the fluid viscosity, ϵ is the fluid permittivity, and $\mathbf{E}_\infty$ is the constant applied electric field. This equation is valid on the basis of several assumptions: (i) the local radii of curvature of the particle are much larger than the thickness of the electric double layer; (ii) the fluid surrounding the particle is unbounded; and (iii) the ζ potential is uniform on the length scale of the particle. The first restriction also implies that the double layer remains approximately in equilibrium despite the migrations of the particle and diffuse ions. Even though many colloidal particles undergoing electrophoresis fulfill this condition, electrophoresis of particles with thick or distorted double layers is encountered in certain cases so that relevant corrections to the Smoluchowski prediction in eq 1 are necessary and have been obtained.[4−8]

In many electrophoresis applications to particle analysis or separation, particles migrate in the vicinity of solid boundaries. For instance, electrophoresis in porous media is applied because the unwanted mix-up caused by natural convection due to Joule heating and nonuniform heat transfer can be avoided. Microporous gels or membranes could even be used to achieve high electric fields and permit separations based on both the size and the charge of the particles.[9] In capillary electrophoresis, gels in the capillary column can minimize particle diffusion, prevent particle adsorption to the capillary walls, and eliminate electroosmosis while serving as the anticonvective medium.[10] Deep electrophoresis penetration and deposition of inert colloidal particles over the interstitial surfaces of porous composites has been

* To whom correspondence should be addressed. E-mail: huan@ntu.edu.tw. Fax: +886-2-23623040.

(1) Smoluchowski, M. V. *Bull. Int. Acad. Sci. Cracovie* **1903**, *8*, 182.
(2) Morrison, F. A. *J. Colloid Interface Sci.* **1970**, *34*, 210.
(3) Anderson, J. L. *Ann. Rev. Fluid Mech.* **1989**, *21*, 61.
(4) Henry, D. C. *Proc. R. Soc. London, Ser. A* **1931**, *133*, 106.
(5) O'Brien, R. W.; White, L. R. *J. Chem. Soc., Faraday Trans. 2* **1978**, *74*, 1607.
(6) O'Brien, R. W. *J. Colloid Interface Sci.* **1983**, *92*, 204.
(7) Keh, H. J.; Chen, S. B. *Langmuir* **1993**, *9*, 1142.
(8) Keh, H. J.; Huang, T. Y. *J. Colloid Interface Sci.* **1993**, *160*, 354.
(9) Jorgenson, J. W. *Anal. Chem.* **1986**, *58*, 743A.
(10) Ewing, A. G.; Wallingford, R. A.; Olefirowicz, T. M. *Anal. Chem.* **1989**, *61*, 292A.

10.1021/la7004002 CCC: $37.00
Published on Web 06/15/2007

suggested in the aerospace industry to protect the composites from burning or deterioration.[11] Another example is the electrophoresis of small particles through a Coulter counter designed not only to count and size the particles but also to determine their ζ potentials.[12] Therefore, the boundary effects on electrophoresis are of great importance and have been studied extensively in the past for various cases of uniformly charged colloidal spheres and boundaries.[13−24]

However, many colloidal particles have heterogeneous surface structure or chemistry and are nonuniformly charged. For example, elementary clay particles are flat disks with edges having a different charge density or ζ potential from the faces. Distributions of surface charge or potential for particles can also result from the aggregation of different species of colloids. Even if a particle is homogeneously charged on its surface, an applied electric field could cause the rearrangement of these charges if they are mobile.[25] A ζ-potential distribution on particle surfaces has been found to lead to colloidal instability; even the average ζ potential should be sufficiently high to keep the suspension stable.[26,27] The electrophoretic motion of a dielectric sphere with a nonuniform ζ potential and a thin electric double layer was first analyzed thoroughly by Anderson,[28] although it had also been discussed to some extent earlier.[29] It was found that, in terms of the multipole moments of the ζ potential, the electrophoretic mobility depends not only on the monopole moment (area-averaged ζ potential) but also on the quadrupole moment, and the dipole moment contributes to particle rotation, which tends to align the particle with the electric field. This analysis was later extended to cases of a nonuniformly charged spherical particle with a double layer of finite thickness[30−33] and a nonuniformly charged nonspherical particle.[34−37] Recently, that particles can have random charge nonuniformity has also been demonstrated experimentally.[38,39]

The electrophoretic motion of nonuniformly charged particles in the vicinity of confining walls could also be encountered in some real situations. In addition to the possible examples mentioned above, an electrophoretic positioning process has been employed in electronic applications for assembling very small individual devices, such as an InGaAs light-emitting diode or a nanowire, which must have all electric contacts available on one surface, onto the contact electrodes of a silicon circuit by biasing the contacts to control the placement of these devices with the required precision.[40,41] However, the boundary effects on the electrophoresis of a charged particle with a nonuniform ζ potential have not yet been investigated.

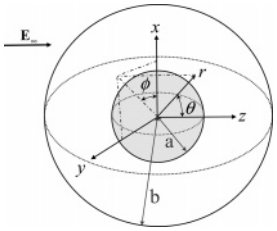

Figure 1. Geometric sketch of the electrophoresis of a colloidal sphere in a concentric spherical cavity.

In this article, we examine the electrophoretic motion of a dielectric sphere situated at the center of a spherical cavity with very thin electric double layers when the surface potentials are arbitrarily nonuniform. The motivation to study this problem arises from the technology of electric paper displays (known as Gyricon displays) where the translation and rotation of each member of an array of hemispherically bichromal, nonuniformly charged balls (about 100 μm in diameter) in its own elastomer-made and solvent-filled spherical cavity (which is only 10−40% larger than the ball) with either a monopole or a dipole on its wall between two thin, transparent plastic sheets are controlled by applying a voltage of either positive or negative polarity across the sheets.[42,43] Although the geometry of the concentric spherical cavity is an idealized abstraction of some other real systems, the result of boundary effects on the electrophoretic velocity of a uniformly charged sphere obtained in this geometry[18] has been shown to be in good agreement with that for a circular cylindrical pore.[19] The geometric symmetry in this model system allows an exact analytical solution to be obtained (as given by eqs 23−28 and illustrated in Figure 2a,b).

2. Analysis

We consider the quasi-steady electrophoretic motion of a nonconducting spherical particle of radius a and ζ potential ζ_p in a concentric spherical cavity (or pore) of radius b and ζ potential ζ_w filled with an electrolyte solution, as illustrated in Figure 1. Both ζ_p and ζ_w can be nonuniform and are taken as arbitrary functions of the position over the particle and cavity surfaces. The applied electric field (or the electric field in the absence of the particle) is constant and equals $E_\infty \mathbf{e}_z$, where $\mathbf{e}_z$ is the unit vector in the positive z (axial) direction. The rectangular coordinates (x, y, z) and spherical coordinates (r, θ, ϕ) are established with their origin at the particle and cavity center. The thickness of the electric double layers adjacent to the particle and cavity surfaces is assumed to be very small relative to the particle radius and the spacing between the solid surfaces. Gravitational effects are ignored. Our objective is to determine the electrophoretic velocity of the particle in the presence of the cavity.

Before determining the electrophoretic velocity of the confined particle with nonuniform ζ_p, the electric potential and velocity fields in the fluid phase must be solved.

2.1. Electric Potential Distribution. The fluid outside the thin double layers is electrically neutral and of constant

(11) Haber, S.; Gal-Or, L. *J. Electrochem. Soc.* **1992**, *139*, 1071.
(12) DeBlois, R. W.; Bean, C. P. *Rev. Sci. Instrum.* **1970**, *41*, 909.
(13) Morrison, F. A.; Stukel, J. J. *J. Colloid Interface Sci.* **1970**, *33*, 88.
(14) Keh, H. J.; Anderson, J. L. *J. Fluid Mech.* **1985**, *153*, 417.
(15) Keh, H. J.; Chen, S. B. *J. Fluid Mech.* **1988**, *194*, 377.
(16) Keh, H. J.; Lien, L. C. *J. Fluid Mech.* **1991**, *224*, 305.
(17) Loewenberg, M.; Davis, R. H. *J. Fluid Mech.* **1995**, *288*, 103.
(18) Zydney, A. L. *J. Colloid Interface Sci.* **1995**, *169*, 476.
(19) Keh, H. J.; Chiou, J. Y. *AIChE J.* **1996**, *42*, 1397.
(20) Keh, H. J.; Jan, J. S. *J. Colloid Interface Sci.* **1996**, *183*, 458.
(21) Ennis, J.; Anderson, J. L. *J. Colloid Interface Sci.* **1997**, *185*, 497.
(22) Yariv, E.; Brenner, H. *Phys. Fluids* **2002**, *14*, 3354.
(23) Yariv, E.; Brenner, H. *J. Fluid Mech.* **2003**, *484*, 85.
(24) Chen, P. Y.; Keh, H. J. *J. Colloid Interface Sci.* **2005**, *286*, 774.
(25) Bazant, M. Z.; Squires, T. M. *Phys. Rev. Lett.* **2004**, *92*, 066101.
(26) Miklavic, S. J.; Chan, D. Y. C.; White, L. R.; Healy, T. W. *J. Phys. Chem.* **1994**, *98*, 9022.
(27) Grant, M. L.; Saville, D. A. *J. Colloid Interface Sci.* **1995**, *171*, 35.
(28) Anderson, J. L. *J. Colloid Interface Sci.* **1985**, *105*, 45.
(29) Teubner, M. *J. Phys. Chem.* **1982**, *76*, 5564.
(30) Yoon, B. J. *J. Colloid Interface Sci.* **1991**, *142*, 575.
(31) Solomentsev, Y. E.; Pawar, Y.; Anderson, J. L. *J. Colloid Interface Sci.* **1993**, *158*, 1.
(32) Velegol, D.; Feick, J. D.; Collins, L. R. *J. Colloid Interface Sci.* **2000**, *230*, 114.
(33) Kim, J. Y.; Yoon, B. J. *J. Colloid Interface Sci.* **2003**, *262*, 101.
(34) Fair, M. C.; Anderson, J. L. *J. Colloid Interface Sci.* **1989**, *127*, 388.
(35) Long, D.; Ajdari, A. *Phys. Rev. Lett.* **1998**, *81*, 1529.
(36) Feick, J. D.; Velegol, D. *Langmuir* **2000**, *16*, 10315.
(37) Kim, J. Y.; Yoon, B. J. *J. Colloid Interface Sci.* **2002**, *251*, 318.
(38) Feick, J. D.; Velegol, D. *Langmuir* **2002**, *18*, 3454.
(39) Feick, J. D.; Chukwumah, N.; Noel, A. E.; Velegol, D. *Langmuir* **2004**, *20*, 3090.
(40) Edman, C. F.; Swint, R. B.; Gurtner, C.; Formosa, R. E.; Roh, S. D.; Lee, K. E.; Swanson, P. D.; Ackley, D. E.; Coleman, J. J.; Heller, M. J. *IEEE Photonics Technol. Lett.* **2000**, *12*, 1198.
(41) Smith, P. A.; Nordquist, C. D.; Jackson, T. N.; Mayer, T. S.; Martin, B. R.; Mbindyo, J.; Mallouk, T. E. *Appl. Phys. Lett.* **2000**, *77*, 1399.
(42) Crawford, G. P. *IEEE Spectrum* **2000**, *37*, 40.

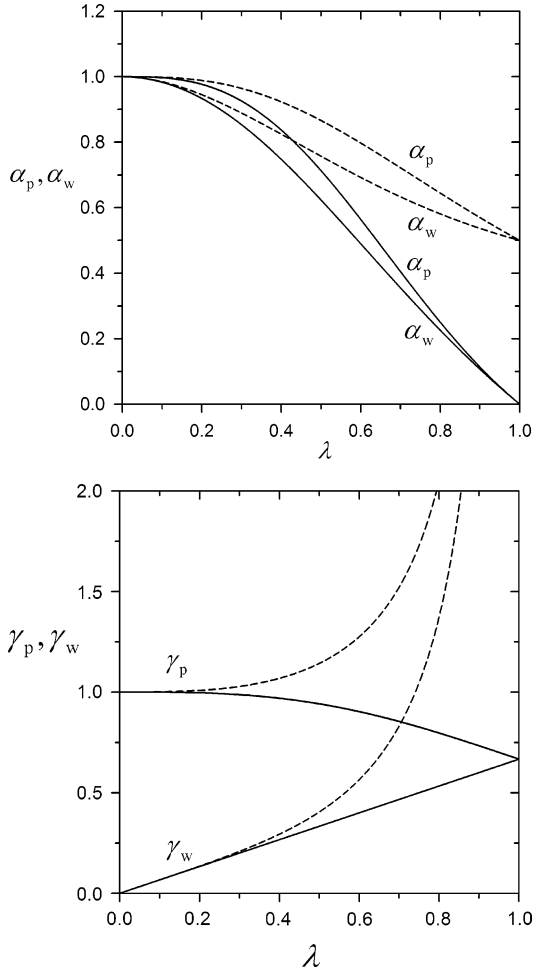

Figure 2. Plots of dimensionless electrophoretic mobility parameters α_p, α_w, γ_p, and γ_w as calculated from eqs 25−28 versus separation parameter λ. The solid curves represent the case using the Dirichlet boundary condition in eq 4, and the dashed curves denote the case using the Neumann boundary condition in eq 6.

conductivity, hence the electric potential distribution $\psi(r, \theta)$ is governed by the Laplace equation,

$$\nabla^2\psi = 0 \tag{2}$$

Because the particle is assumed to be perfectly insulating, the boundary condition for ψ at the surface of the particle is

$$\frac{\partial\psi}{\partial r} = 0 \text{ at } r = a \tag{3}$$

At the surface of the cavity, the electric potential distribution gives rise to the applied electric field when the particle does not exist. Thus, a reasonable choice of the boundary condition there is

$$\psi = -E_\infty r\cos\theta \text{ at } r = b \tag{4}$$

Here, we have set $\psi = 0$ on the plane $z = 0$ for convenience without the loss of generality. The solution of eq 2 subject to these boundary conditions is

$$\psi = -\frac{2E_\infty}{2+\lambda^3}\left(r + \frac{a^3}{2r^2}\right)\cos\theta \tag{5}$$

where $\lambda = a/b$.

(43) Crowley, J. M.; Sheridon, N. K.; Romano, L. *J. Electrost.* **2002**, *55*, 247.

The boundary condition at the cavity wall may alternatively be taken that the local electric potential gradient is equal in magnitude to the prescribed electric field. In this case, the Dirichlet approach given by eq 4 becomes the following Neumann approach:[18,44]

$$\frac{\partial\psi}{\partial r} = -E_\infty\cos\theta \text{ at } r = b \tag{6}$$

Note that although the normal component of the electric potential gradient at the cavity wall given by this boundary condition is consistent with the applied electric field its tangential (angular) component is not specified. The solution of eq 2 subject to eq 3 and boundary condition 6 is given by

$$\psi = -\frac{E_\infty}{1-\lambda^3}\left(r + \frac{a^3}{2r^2}\right)\cos\theta \tag{7}$$

In fact, eq 5 predicts that the electric potential at the particle surface ($r = a$) is decreased by the presence of the cavity by a factor of $(1 + \lambda^3/2)^{-1}$, whereas eq 7 suggests that this potential is increased by a factor of$(1 - \lambda^3)^{-1}$. In the limit $\lambda \to 0$, as expected, eqs 5 and 7 become identical and reduce to the potential distribution for a nonconducting sphere in an unbounded medium.

2.2. Fluid Velocity Distribution. Having obtained the solution for the electric potential distribution, we can now proceed to find the fluid velocity field. Because the Reynolds number is small, the fluid motion outside the thin electric double layers is governed by the Stokes equations,

$$\eta\nabla^2\mathbf{v} - \nabla p = \mathbf{0} \tag{8}$$

$$\nabla\cdot\mathbf{v} = 0 \tag{9}$$

The general solution of the above equations is given by[45,46]

$$\mathbf{v} = \sum_{n=-\infty}^{\infty}\left[\nabla\times(\mathbf{r}\chi_n) + \nabla\Phi_n + \frac{n+3}{2\eta(n+1)(2n+3)}r^2\nabla p_n - \frac{n}{\eta(n+1)(2n+3)}\mathbf{r}p_n\right] \tag{10}$$

$$p = \sum_{n=-\infty}^{\infty} p_n \tag{11}$$

where $p_n(\mathbf{r})$, $\Phi_n(\mathbf{r})$, and $\chi_n(\mathbf{r})$ are solid spherical harmonics of order n and $\mathbf{r}$ is the position vector.

Because the electric field acting on the diffuse ions within the thin double layer at each solid surface produces a relative tangential fluid velocity at the outer edge of the double layer as given by the Helmholtz[47] expression for the electroosmotic flow, the boundary conditions for the fluid velocity require that

$$\mathbf{v} = \mathbf{v}_s^p = \mathbf{U} + a\Omega\times\mathbf{n} + \frac{\epsilon\zeta_p}{\eta}(\mathbf{I} - \mathbf{nn})\cdot\nabla\psi \text{ at } r = a \tag{12}$$

$$\mathbf{v} = \mathbf{v}_s^w = \frac{\epsilon\zeta_w}{\eta}(\mathbf{I} - \mathbf{nn})\cdot\nabla\psi \text{ at } r = b \tag{13}$$

Here, $\mathbf{U}$ and Ω are the translational and angular velocities,

(44) Jackson, J. D. *Classical Electrodynamics*, 2nd ed.; John Wiley & Sons: New York, 1976; Chapter 1.
(45) Lamb, H. *Hydrodynamics*; Dover: New York, 1945.
(46) Happel, J.; Brenner, H. *Low Reynolds Number Hydrodynamics*; Martinus Nijhoff: Dordrecht, The Netherlands, 1983.
(47) Helmholtz, H. *Ann.* **1879**, *7*, 337.

respectively, of the electrophoretic sphere to be determined, **n** is the unit normal vector on the particle surface pointing toward the fluid phase, **I** is the unit dyadic, and the expression for ψ has already been given by eq 5 or 7.

As it can be shown,[46] to get the solutions of eqs 8 and 9 in the form of eqs 10 and 11 with boundary conditions given by eqs 12 and 13 for a spherical particle in a concentric spherical cavity, the solid spherical harmonic functions can be calculated from the relationships

$$\mathbf{n}\cdot\mathbf{v}_s^{p,w} = \sum_{n=0}^{\infty} X_n^{p,w} = \sum_{n=-\infty}^{\infty}\left[\frac{n a_{p,w}}{2\eta(2n+3)}\left(\frac{a_{p,w}}{r}\right)^n p_n + \frac{n}{a_{p,w}}\left(\frac{a_{p,w}}{r}\right)^n \Phi_n\right] \quad (14)$$

$$-a_{p,w}\nabla\cdot\mathbf{v}_s^{p,w} = \sum_{n=0}^{\infty} Y_n^{p,w} = \sum_{n=-\infty}^{\infty}\left[\frac{n(n+1)a_{p,w}}{2\eta(2n+3)}\left(\frac{a_{p,w}}{r}\right)^n p_n + \frac{n(n-1)}{a_{p,w}}\left(\frac{a_{p,w}}{r}\right)^n \Phi_n\right] \quad (15)$$

$$a_{p,w}\mathbf{n}\cdot(\nabla\times\mathbf{v}_s^{p,w}) = \sum_{n=0}^{\infty} Z_n^{p,w} = \sum_{n=-\infty}^{\infty}\left[n(n+1)\left(\frac{a_{p,w}}{r}\right)^n \chi_n\right] \quad (16)$$

Here, $X_n^{p,w}(\theta, \phi)$, $Y_n^{p,w}(\theta, \phi)$, and $Z_n^{p,w}(\theta, \phi)$ are the surface spherical harmonics, the superscripts or subscripts p and w represent the surfaces of the particle and cavity, respectively, $\mathbf{v}_s^{p,w}$ represents the fluid velocity distributions on the corresponding surfaces given by eqs 12 and 13, $a_p = a$, and $a_w = b$. From the second part of eqs 14−16, the relations between the solid spherical harmonics (p_n, Φ_n, χ_n) and the surface spherical harmonics ($X_n^{p,w}$, $Y_n^{p,w}$, $Z_n^{p,w}$) can be obtained, and they are given by eqs A1−A9 in Appendix A.

The ζ potentials ζ_p and ζ_w are arbitrary functions of (θ, ϕ) and can be expressed in terms of the multipole expansions,[28,37]

$$\zeta_{p,w} = M^{p,w} + 3\mathbf{D}^{p,w}\cdot\mathbf{n} + \frac{5}{2}\mathbf{Q}^{p,w}:\mathbf{nn} \quad (17)$$

Here the monopole, dipole, and quadrupole moments $M^{p,w}$, $\mathbf{D}^{p,w}$, and $\mathbf{Q}^{p,w}$, respectively, are defined by the following integrals over the particle and cavity surfaces $S^{p,w}$

$$M^{p,w} = \frac{1}{S^{p,w}}\int_{S^{p,w}} \zeta_{p,w}\, dS \quad (18)$$

$$\mathbf{D}^{p,w} = \frac{1}{S^{p,w}}\int_{S^{p,w}} \zeta_{p,w}\mathbf{n}\, dS \quad (19)$$

$$\mathbf{Q}^{p,w} = \frac{1}{S^{p,w}}\int_{S^{p,w}} \zeta_{p,w}(3\mathbf{nn} - \mathbf{I})\, dS \quad (20)$$

and the higher-order moments (which make no contribution to the electrophoretic velocity of the particle, as will be discussed later) are neglected. Various nonuniform ζ potentials $\zeta_{p,w}$ can result from eq 17 with appropriate choices of moments $M^{p,w}$ (i.e., area-averaged ζ potentials), $\mathbf{D}^{p,w}$, and $\mathbf{Q}^{p,w}$ (which are symmetric and traceless).

With the substitution of the surface velocities given by eqs 12 and 13, in which the electric potential is given by eq 5 or 7 and the ζ potentials are expressed by eq 17, into the first part of eqs 14−16, the surface spherical harmonics $X_n^{p,w}$, $Y_n^{p,w}$, and $Z_n^{p,w}$ can be calculated in terms of the components of moments $M^{p,w}$, $\mathbf{D}^{p,w}$, and $\mathbf{Q}^{p,w}$. It is found that $X_n^{p,w} = 0$ for all n, and the nonzero contributions of harmonic functions $Y_n^{p,w}$ and $Z_n^{p,w}$ are given by eqs A10−A14. For the electrophoresis of a sphere in a concentric spherical cavity with specified ζ-potential distributions, the fluid flow field can be obtained as an explicit function of the components of moments $M^{p,w}$, $\mathbf{D}^{p,w}$, and $\mathbf{Q}^{p,w}$ using eqs 10, 11, and A1−A14.

The force **F** and torque **T** exerted by the fluid on the particle as a result of the electrokinetic motion can be determined from[46]

$$\mathbf{F} = -4\pi\nabla(r^3 p_{-2}) \quad (21)$$

$$\mathbf{T} = -8\pi\eta\nabla(r^3\chi_{-2}) \quad (22)$$

These equations indicate that only low-order solid harmonic functions p_{-2} and χ_{-2} contribute to the hydrodynamic force and torque on the particle. Note that p_{-2} and χ_{-2} are functions of monopole, dipole, and quadrupole moments $M^{p,w}$, $\mathbf{D}^{p,w}$, and $\mathbf{Q}^{p,w}$ of the ζ-potential distributions but are independent of their higher-order moments.

2.3. Derivation of the Particle Velocities. At the quasi-steady state, the net force and net torque acting on the electrophoretic particle must vanish. Applying these constraints to eqs 21 and 22 and using eqs A2 and A6 (taking $n = 1$, $X_n^{p,w} = 0$, and $Y_n^{p,w}$and $Z_n^{p,w}$ as given by eqs A10 and A13) for harmonic functions p_{-2} and χ_{-2}, we obtain the translational and angular velocities of the particle in the cavity as

$$\mathbf{U} = \frac{\epsilon}{\eta}\left[\alpha_p\left(M^p\mathbf{I} - \frac{1}{2}\mathbf{Q}^p\right) + \alpha_w\left(M^w\mathbf{I} - \frac{1}{2}\mathbf{Q}^w\right)\right]\cdot\mathbf{E}_\infty \quad (23)$$

$$\mathbf{\Omega} = \frac{9\epsilon}{4\eta a}[\gamma_p\mathbf{D}^p - \gamma_w\mathbf{D}^w]\times\mathbf{E}_\infty \quad (24)$$

where

$$\alpha_p = \frac{2 - 5\lambda^3 + 3\lambda^5}{\nu(1-\lambda^5)} \quad (25)$$

$$\alpha_w = \frac{6 - 10\lambda^2 + 3\lambda^3 - \lambda^5 + 2\lambda^8}{3\nu(1-\lambda^5)} \quad (26)$$

$$\gamma_p = \frac{2}{\nu} \quad (27)$$

$$\gamma_w = \frac{2}{3\nu}\lambda(2+\lambda^3) \quad (28)$$

and $\nu = 2 + \lambda^3$ if the Dirichlet boundary condition in eq 4 is employed, whereas $\nu = 2(1 - \lambda^3)$ if the Neumann boundary condition in eq 6 is used. Note that all four parameters α_p, α_w, γ_p, and γ_w given by eqs 25−28 are functions of the ratio $\lambda = {}^a/_b$ alone. Although the expressions for the particle velocities in eqs 23 and 24 involve only the monopole, dipole, and quadrupole moments of the ζ potentials, they are exact for a particle-in-cavity system with arbitrary ζ potential distributions because the higher-order moments make no contribution to the particle velocities.

For the electrophoresis of a colloidal sphere in a concentric spherical cavity with specified ζ-potential distributions, eqs 23 and 24 together with eqs 25−28 can be easily used to determine

the particle velocities after the calculation of the multipole moments of the ζ-potential distributions according to eqs 18−20. The translational velocity of the particle depends only on the monopole and quadrupole moments of the ζ-potential distributions at the particle and cavity surfaces (the existence of the quadrupole moments results in an anisotropic electrophoretic mobility of the particle), whereas the rotational velocity is affected only by the dipole moments. The effect of finite values of parameters α_w and γ_w is due to the electroosmotic flow that arises from the interaction between the imposed electric field and the thin double layer adjacent to the cavity wall. Equations 23 and 24 indicate that the contributions from the wall-corrected electrophoretic driving force (involving parameters α_p and γ_p) and the electroosmotic flow to the particle velocities can be superimposed, which is due to the linearity of the problem. Note that the dependence of α_p and α_w on λ is different in order, and so is that for parameters γ_p and γ_w.

It can be found that all four parameters α_p, α_w, γ_p, and γ_w given by eqs 25−28 are always positive as long as $0 < \lambda < 1$. In the limit of $\lambda \to 0$, eqs 25−28 reduce to $\alpha_p = \alpha_w = \gamma_p = 1$ and $\gamma_w = 0$, in which the electrophoretic and angular velocities for an unconfined dielectric sphere with nonuniform ζ_p obtained by Anderson[28]

$$\mathbf{U}_0 = \frac{\epsilon}{\eta}\left(M^p\mathbf{I} - \frac{1}{2}\mathbf{Q}^p\right)\cdot\mathbf{E}_\infty \tag{29}$$

$$\Omega_0 = \frac{9\epsilon}{4\eta a}\mathbf{D}^p \times \mathbf{E}_\infty \tag{30}$$

are reproduced (with the effect of the electroosmotic flow arising from the interaction of the prescribed electric field with the charged cavity at infinity given by $\alpha_w = 1$ excluded). When ζ_p is uniform over the particle surface, eqs 29 and 30 reduce to eq 1 and $\Omega_0 = \mathbf{0}$. In the limit of $\lambda \to 1$, eqs 25−28 become $\alpha_p = \alpha_w = 0$ and $\gamma_p = \gamma_w = {}^2/_3$ if the boundary condition in eq 4 is adopted for the electric potential at the cavity wall, and $\alpha_p = \alpha_w = {}^1/_2$ and $\gamma_p = \gamma_w \to \infty$ if the boundary condition in eq 6 is used. Note that eqs 25 and 26 for α_p and α_w with $\nu = 2(1 - \lambda^3)$ are identical to the corresponding equations derived by Zydney[18] for a uniformly charged spherical particle undergoing electrophoretic motion in a uniformly charged concentric spherical cavity using the boundary condition in eq 6. For a given finite value of λ, the values of parameters α_p, α_w, γ_p, and γ_w predicted using eq 4 are always smaller than their corresponding results obtained using eq 6.

In terms of the electrophoretic and angular velocities for an isolated dielectric sphere given by eqs 29 and 30, it is convenient to express the bounded result of eqs 23 and 24 as the normalized velocity components in rectangular coordinates,

$$\frac{U_i}{U_{0i}} = \alpha_p + \alpha_w k_i \tag{31}$$

$$\frac{\Omega_i}{\Omega_{0i}} = \gamma_p + \gamma_w l_i \tag{32}$$

where

$$k_i = \frac{\left[\left(M^w\mathbf{I} - \frac{1}{2}\mathbf{Q}^w\right)\cdot\mathbf{E}_\infty\right]_i}{\left[\left(M^p\mathbf{I} - \frac{1}{2}\mathbf{Q}^p\right)\cdot\mathbf{E}_\infty\right]_i} \tag{33}$$

$$l_i = -\frac{[\mathbf{D}^w \times \mathbf{E}_\infty]_i}{[\mathbf{D}^p \times \mathbf{E}_\infty]_i} \tag{34}$$

and subscript i represents the x, y, or z component for which the unbounded velocity U_{i0} or Ω_{i0} is nonzero. Parameters k_i and l_i correspond to the strength of the electroosmotic flow that develops from the interaction between the imposed electric field and the thin double layer adjacent to the cavity wall relative to the electrophoretic driving force when the cavity wall is at infinity. These two parameters can be either positive or negative (meaning that the contributions to the particle velocities from the cavity-induced electroosmotic flow can be in either the same or in the opposite direction to those from the electrophoretic driving force), depending on the combination of the ζ-potential distributions at the particle and cavity surfaces. Equations 31 and 32 show that the i component of the normalized electrophoretic velocity of the spherical particle depends only on parameters α_p, α_w, and k_i and the i component of the normalized angular velocity depends only on γ_p, γ_w, and l_i. Note that for a specified component i in a bounded system it is possible that U_i (or Ω_i) is finite while U_{0i} (or Ω_{0i}) vanishes.

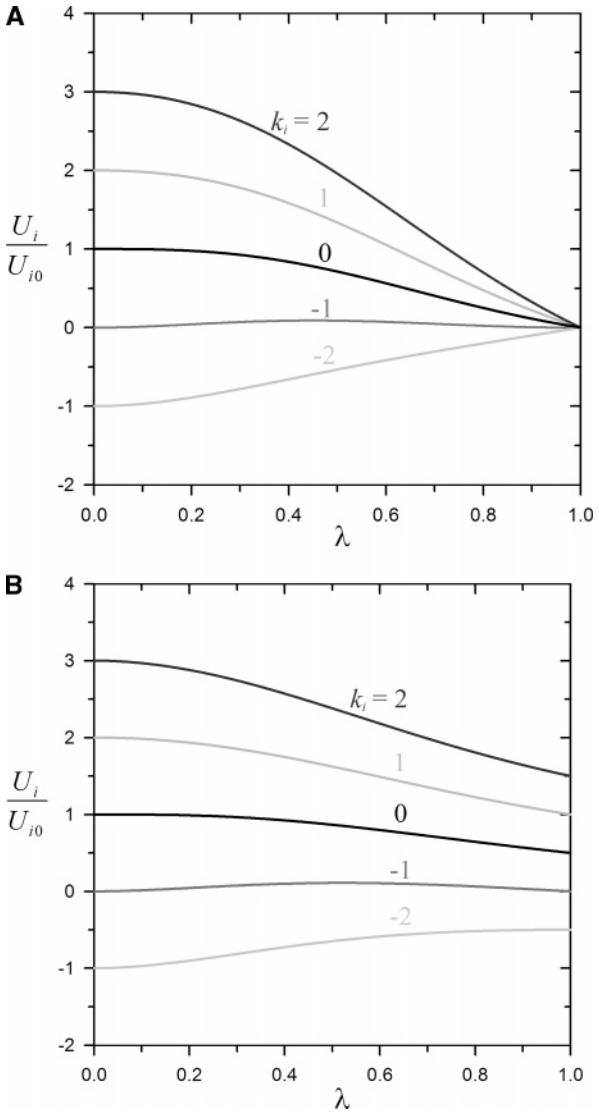

Figure 3. Plots of normalized translational velocity U_i/U_{0i} of the electrophoretic particle versus separation parameter λ: (a) the case using the Dirichlet boundary condition in eq 4 and (b) the case using the Neumann boundary condition in eq 6.

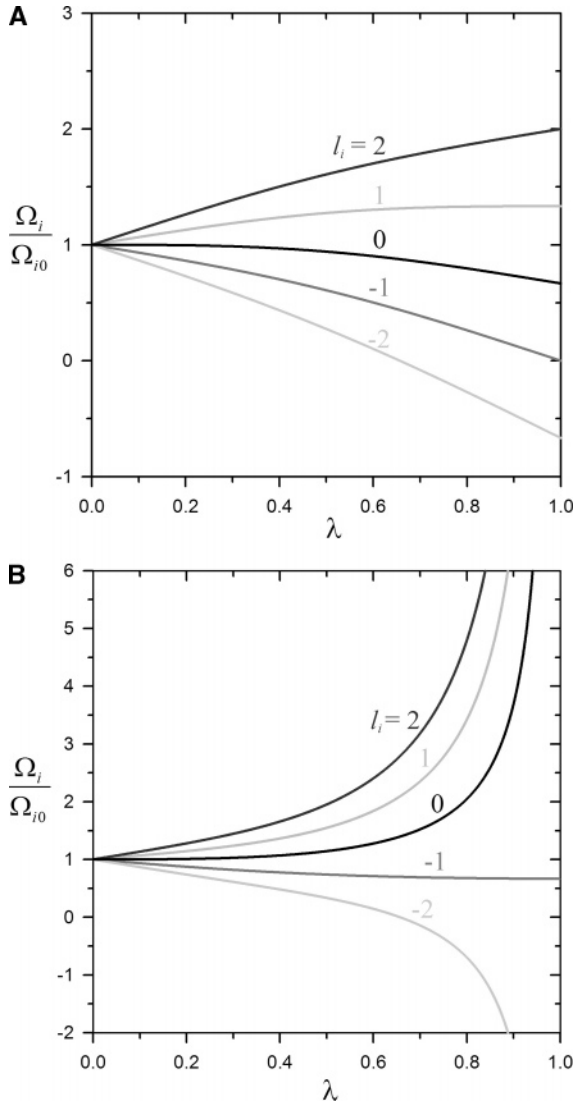

Figure 4. Plots of normalized angular velocity Ω_i/Ω_{0i} of the electrophoretic particle versus separation parameter λ: (a) the case using the Dirichlet boundary condition in eq 4 and (b) the case using the Neumann boundary condition in eq 6.

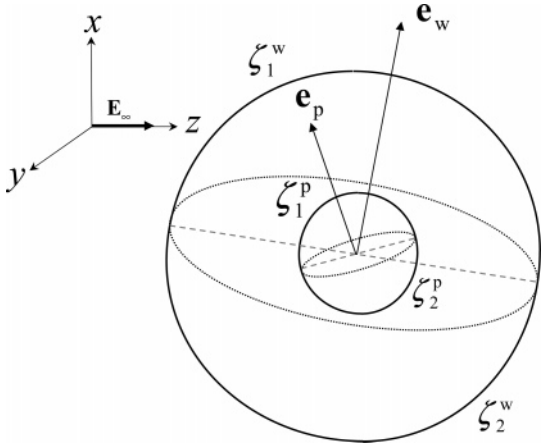

Figure 5. Geometric sketch of the electrophoresis of a colloidal sphere with an odd ζ-potential distribution formed by one hemisphere of the constant value ζ_1^p attached to a second hemisphere of ζ_2^p in a concentric spherical cavity with an odd ζ-potential distribution formed by one hemisphere of ζ_1^w attached to a second hemisphere of ζ_2^w. The $z-x$ plane is chosen to contain both unit vector $\mathbf{e}_p$ defining the axis of rotational symmetry of the particle and applied electric field $\mathbf{E}_\infty$.

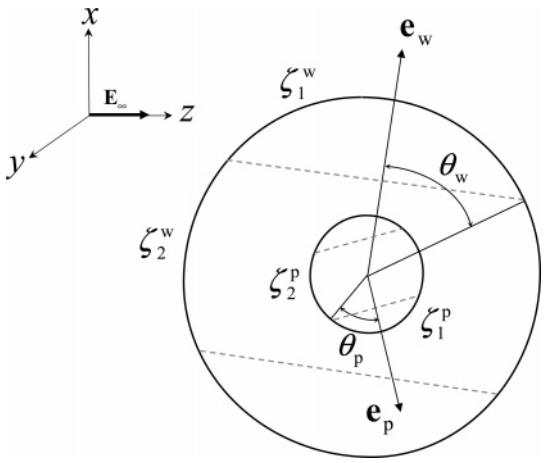

Figure 6. Geometric sketch of the electrophoresis of a colloidal sphere with an even ζ-potential distribution formed by two caps of the constant value ζ_1^p and a middle of ζ_2^p in a concentric spherical cavity with an even ζ-potential distribution formed by two caps of ζ_1^w and a middle of ζ_2^w. The $z-x$ plane is chosen to contain both unit vector $\mathbf{e}_p$ defining the axis of rotational symmetry of the particle and applied electric field $\mathbf{E}_\infty$.

3. Results and Discussion

The numerical values of dimensionless mobility parameters α_p, α_w, γ_p, and γ_w of a spherical particle undergoing electrophoresis in a concentric spherical cavity, as calculated from eqs 25−28, are plotted versus separation parameter λ in Figure 2a,b. It can be seen that both α_p and α_w are monotonically decreasing functions of λ from unity at $\lambda = 0$ to zero (if the Dirichlet boundary condition in eq 4 is adopted for the electric potential at the cavity wall) or to $^1/_2$ (if the Neumann boundary condition in eq 6 is used) at $\lambda = 1$. Thus, the net effect of the approach of the cavity wall to the particle, dominated by the contribution from viscous retardation, is to reduce both the electrophoretic driving force and the cavity-induced electroosmotic sweeping force on the particle. However, γ_w is a monotonically increasing function of λ from zero at $\lambda = 0$ to $^2/_3$ (if eq 4 is adopted) or to infinity (if eq 6 is used) at $\lambda = 1$, whereas interestingly γ_p decreases monotonically with an increase in λ from unity at $\lambda = 0$ to $^2/_3$ at $\lambda = 1$ (if eq 4 is adopted) or increases monotonically with λ from unity at $\lambda = 0$ to infinity at $\lambda = 1$ (if eq 6 is used). Note that for any given value of λ between 0 and 1, α_p is greater than α_w and γ_p is greater than γ_w, no matter whether eq 4 or 6 is used for the boundary condition of the electric potential at the cavity wall.

The normalized velocities U_i/U_{0i} and Ω_i/Ω_{0i} calculated from eqs 31 and 32 as functions of λ are depicted in Figures 3 and 4, respectively, for various values of k_i and l_i. For a constant value of λ, as expected, the value of U_i/U_{0i} increases monotonically with an increase in k_i, and the value of Ω_i/Ω_{0i} increases monotonically with an increase in l_i. As long as the values of k_i and l_i are greater than -1, the values of U_i/U_{0i} and Ω_i/Ω_{0i}, respectively, are always positive. When the values of k_i and l_i are smaller than about -1, however, the values of U_i/U_{0i} and Ω_i/Ω_{0i} may become negative, meaning that the translational and rotational velocities of the particle may reverse their directions because of the relatively strong effect of the cavity-induced

electroosmotic flow in the opposite direction at the center of the cavity. For specified values of k_i and l_i, the magnitude of U_i/U_{0i} in general decreases with an increase in λ (with exceptions when k_i equals about -1), whereas the magnitude of $\Omega_i/\Omega_{0i} - 1$ increases with an increase in λ. For given finite values of k_i and λ, the magnitude of U_i/U_{0i} predicted from using the Neumann boundary condition in eq 6 in general is greater than that predicted from using the Dirichlet boundary condition in eq 4.

As an example, we consider the electrophoresis of a colloidal sphere with an odd ζ-potential distribution formed by one hemisphere of the constant value ζ_1^p attached to a second hemisphere of ζ_2^p in a concentric spherical cavity similarly composed of two hemispheres of different constant ζ potentials ζ_1^w and ζ_2^w, as shown in Figure 5. Unit vectors $\mathbf{e}_p$ and $\mathbf{e}_w$ define the axes of rotational symmetry of the particle and cavity, respectively, and both are allowed to orient arbitrarily with respect to the applied electric field $\mathbf{E}_\infty$. The $z-x$ plane is chosen to contain both $\mathbf{e}_p$ and $\mathbf{E}_\infty$. After calculating the multipole moments according to eqs 18−20 and substituting their result into eqs 23 and 24, we obtain

$$\mathbf{U} = \frac{\epsilon}{2\eta}[\alpha_p(\zeta_1^p + \zeta_2^p) + \alpha_w(\zeta_1^w + \zeta_2^w)]\mathbf{E}_\infty \quad (35)$$

$$\mathbf{\Omega} = \frac{9\epsilon}{16\eta a}[\gamma_p(\zeta_1^p - \zeta_2^p)\mathbf{e}_p - \gamma_w(\zeta_1^w - \zeta_2^w)\mathbf{e}_w] \times \mathbf{E}_\infty \quad (36)$$

Because the quadrupole moments disappear and the higher-order moments do not contribute in this case, eq 35 shows that the electrophoretic velocity of the particle is always collinear with the applied electric field, irrespective of the orientations of $\mathbf{e}_p$ and $\mathbf{e}_w$. The cavity wall can induce an angular velocity of the particle with both x and y components, although the particle rotates only about the y axis in the absence of the cavity.

For another example in contrast to the previous one, we consider the electrophoresis of a colloidal sphere with an even ζ-potential distribution formed by two caps of the constant value ζ_1^p connected by a middle section of ζ_2^p in a concentric spherical cavity with a similar even ζ-potential distribution formed by two caps of ζ_1^w and a middle of ζ_2^w, as shown in Figure 6. Again, the orientations of the axes of rotational symmetry of the particle and cavity, given by unit vectors $\mathbf{e}_p$ and $\mathbf{e}_w$, respectively, can be arbitrary relative to the imposed electric field $\mathbf{E}_\infty$, and the z-x plane is chosen to contain both $\mathbf{e}_p$ and $\mathbf{E}_\infty$. Using eqs 18−20 for this case, we find that

$$M^{p,w} = \zeta_2^{p,w}\cos\theta_{p,w} + \zeta_1^{p,w}(1 - \cos\theta_{p,w}) \quad (37)$$

$$\mathbf{Q}^{p,w} = \frac{1}{2}(\zeta_1^{p,w} - \zeta_2^{p,w})(\cos\theta_{p,w} - \cos^3\theta_{p,w})(3\mathbf{e}_{p,w}\mathbf{e}_{p,w} - \mathbf{I}) \quad (38)$$

and the dipole moments of the ζ potentials at the particle and cavity surfaces vanish. In this case, the electroosmotic flow that arises from the interaction between the applied electric field and the thin double layer adjacent to the cavity wall may contribute to the translational velocity of the particle in all three rectangular components, whereas the contribution from the electrophoretic driving force has only z and x components. The particle is irrotational without the contribution from the dipole moments. When the values of angles $\theta_{p,w} = 0$ or $\pi/2$, the ζ-potential distributions are uniform, and the result of eqs 23 and 24 with eqs 37 and 38 reduces to that for a uniformly charged spherical particle undergoing electrophoretic motion in a uniformly charged concentric spherical cavity.

4. Concluding Remarks

The quasi-steady electrophoretic motion of a dielectric sphere in a concentric spherical cavity with arbitrary ζ-potential distributions at the particle and cavity surfaces has been theoretically investigated in this study. The applied electric field is constant, and the thickness of the electric double layers adjacent to the solid surfaces is assumed to be much smaller than the particle radius and the gap width between the surfaces. Both the Dirichlet-type and the Neumann-type boundary conditions are considered for the electric potential at the cavity wall. The Laplace and Stokes equations are solved analytically for the electric potential and velocity fields, respectively, in the fluid phase, and the translational and angular velocities of the electrophoretic particle are obtained in explicit expressions, eqs 23 and 24, with the relevant parameters (functions of the ratio of the particle-to-cavity radii only) given by eqs 25−28 and Figure 2a,b. Before using these equations, one has to evaluate only the monopole, dipole, and quadrupole moments of the ζ-potential distributions at the particle and cavity surfaces defined by eqs 18−20. The contributions from the electroosmotic flow arising from the interaction of the applied electric field with the thin double layer adjacent to the cavity wall and from the wall-corrected electrophoretic driving force to the particle velocities can be superimposed because of the linearity of the problem. Two examples of the particle−cavity system with odd and even ζ-potential distributions, respectively, are given so that we may discuss in detail the boundary effects of the cavity on the electrophoretic velocities of the particle.

We note that the two types of boundary conditions for the electric potential at the cavity wall lead to somewhat different results for the translational and rotational velocities of the electrophoretic particle. These two boundary conditions have also been used in the literature to study the electrophoresis of a suspension of colloidal spheres with thin electric double layers using the unit cell model.[48−51] The results of these studies indicate that the tendency of the dependence of the mean electrophoretic mobility on the volume fraction of the particles predicted by the Neumann type is not as correct as that predicted by the Dirichlet type in comparison with the ensemble-averaged results obtained by using the concept of statistical mechanics. Therefore, the boundary condition represented by eq 6 might not be as accurate as that represented by eq 4, probably because of the fact that the angular component of the electric potential gradient at the cavity wall is not specified in eq 6.

Appendix A

Relations among the Solid Spherical Harmonics, Surface Spherical Harmonics, and Multipole Moments of Zeta Potential Distributions Obtained from Equations 12−17. The relations between the nonzero solid spherical harmonics (p_n, Φ_n, χ_n) and the surface spherical harmonics ($X_n^{p,w}$, $Y_n^{p,w}$, $Z_n^{p,w}$) obtained from eqs 14−16 are

(48) Levine, S.; Neale, G. H. *J. Colloid Interface Sci.* **1974**, *47*, 520.
(49) Zharkikh, N. I.; Shilov, V. N. *Colloid J. USSR* (English Translation) **1982**, *43*, 865.
(50) Kozak, M. W.; Davis, E. J. *J. Colloid Interface Sci.* **1989**, *127*, 497.
(51) Wei, Y. K.; Keh, H. J. *Langmuir* **2001**, *17*, 1437.

$$p_n = \frac{2\eta(2n+3)}{na\Gamma_n(\lambda)}\left(\frac{r}{a}\right)^n \lambda^{n+2}\{\lambda^n[(n+2)(2n-1) - n(2n+1)\lambda^2 - 2(n-1)\lambda^{2n+1}]X_n^p + [-2(n-1) - n(2n+1)\lambda^{2n-1} + (n+2)(2n-1)\lambda^{2n+1}]X_n^w + \lambda^n[2n-1-(2n+1)\lambda^2 + 2\lambda^{2n+1})]Y_n^p + [2-(2n+1)\lambda^{2n-1} + (2n-1)\lambda^{2n+1}]Y_n^w\} \quad (A1)$$

$$p_{-n-1} = \frac{2\eta(2n-1)}{(n+1)a\Gamma_n(\lambda)}\left(\frac{r}{a}\right)^{-n-1}\{\lambda[2(n+2) + (n-1)(2n+3)\lambda^{2n+1} - (n+1)(2n+1)\lambda^{2n+3}]X_n^p + \lambda^n[-(n+1)(2n+1) + (n-1)(2n+3)\lambda^2 + 2(n+2)\lambda^{2n+3}]X_n^w + \lambda[2-(2n+3)\lambda^{2n+1} + (2n+1)\lambda^{2n+3}]Y_n^p + \lambda^n[2n+1-(2n+3)\lambda^2 + 2\lambda^{2n+3}]Y_n^w\} \quad (A2)$$

$$\Phi_n = \frac{a}{n\Gamma_n(\lambda)}\left(\frac{r}{a}\right)^n \lambda^n\{\lambda^n[-(n+2)(2n+1) + n(2n+3)\lambda^2 + 2(n+1)\lambda^{2n+3}]X_n^p + [2(n+1) + n(2n+3)\lambda^{2n+1} - (n+2)(2n+1)\lambda^{2n+3})]X_n^w + \lambda^n[-(2n+1) + (2n+3)\lambda^2 - 2\lambda^{2n+3}]Y_n^p + [-2 + (2n+3)\lambda^{2n+1} - (2n+1)\lambda^{2n+3}]Y_n^w\} \quad (A3)$$

$$\Phi_{-n-1} = \frac{a}{(n+1)\Gamma_n(\lambda)}\left(\frac{r}{a}\right)^{-n-1}\{\lambda[2n + (n-1)(2n+1)\lambda^{2n-1} - (n+1)(2n-1)\lambda^{2n+1})]X_n^p + \lambda^n[-(n+1)(2n-1) + (n-1)(2n+1)\lambda^2 + 2n\lambda^{2n+1}]X_n^w + \lambda[2-(2n+1)\lambda^{2n-1} + (2n-1)\lambda^{2n+1})]Y_n^p + \lambda^n[2n-1-(2n+1)\lambda^2 + 2\lambda^{2n+1}]Y_n^w\} \quad (A4)$$

$$\chi_n = \frac{-\lambda^{2n+1}Z_n^p + \lambda^n Z_n^w}{1-\lambda^{2n+1}} \quad (A5)$$

$$\chi_{-n-1} = \frac{Z_n^p - \lambda^n Z_n^w}{1-\lambda^{2n+1}} \quad (A6)$$

for $n \geq 1$, and

$$p_{-1} = -\frac{\eta}{r}(2X_0^w + Y_0^w) \quad (A7)$$

$$\Phi_{-1} = \frac{a^2}{2r\lambda^2}Y_0^w \quad (A8)$$

where

$$\Gamma_n(\lambda) = 4\lambda(1+\lambda^{4n+2}) - \lambda^{2n}[(2n+1)^2(1+\lambda^4) - 2(2n-1)(2n+3)\lambda^2] \quad (A9)$$

The expressions for the nonzero surface spherical harmonics $X_n^{p,w}$, $Y_n^{p,w}$, and $Z_n^{p,w}$ in terms of the components of multipole moments $M^{p,w}$, $\mathbf{D}^{p,w}$, and $\mathbf{Q}^{p,w}$ of the ζ-potential distributions at the particle and cavity surfaces in rectangular coordinates (x, y, z) obtained from eqs 12−17 are

$$Y_1^{p,w} = \beta^{p,w}[(-2M^{p,w} + Q_{zz}^{p,w})\cos\theta + (Q_{yz}^{p,w}\sin\phi + Q_{xz}^{p,w}\cos\phi)\sin\theta] \quad (A10)$$

$$Y_2^{p,w} = -3\beta^{p,w}[D_z^{p,w}(3\cos^2\theta - 1) + 3(D_y^{p,w}\sin\phi + D_x^{p,w}\cos\phi)\cos\theta\sin\theta] \quad (A11)$$

$$Y_3^{p,w} = -\beta^{p,w}[3Q_{zz}^{p,w}(5\cos^3\theta - 3\cos\theta) + 4(Q_{yz}^{p,w}\sin\phi + Q_{xz}^{p,w}\cos\phi)(5\cos^2\theta - 1)\sin\theta + 5(2Q_{xy}^{p,w}\sin 2\phi - (Q_{yy}^{p,w} - Q_{xx}^{p,w})\cos 2\phi)\cos\theta\sin^2\theta] \quad (A12)$$

$$Z_1^{p,w} = 3\beta^{p,w}(D_x^{p,w}\sin\phi - D_y^{p,w}\cos\phi)\sin\theta \quad (A13)$$

$$Z_2^{p,w} = 5\beta^{p,w}\{(Q_{xz}^{p,w}\sin\phi - Q_{yz}^{p,w}\cos\phi)\cos\theta\sin\theta - \left[\frac{1}{2}(Q_{yy}^{p,w} - Q_{xx}^{p,w})\sin 2\phi + Q_{xy}^{p,w}\cos 2\phi\right]\sin^2\theta\} \quad (A14)$$

where $\beta^p = {}^3/_\nu$, $\beta^w = 1$, and ν is defined right after eq 28.

Acknowledgment. This research was partially supported by the National Science Council of the Republic of China.

LA7004002